QUANTITATIVE AUTORADIOGRAPHIC STUDY OF LABELED RNA IN RABBIT OPTIC NERVE AFTER INTRAOCULAR INJECTION OF [^{3}H]URIDINE

PIERLUIGI GAMBETTI, LUCILA AUTILIO-GAMBETTI, BRENDA SHAFER, and LADORNA PFAFF

From the Division of Neuropathology, University of Pennsylvania, Philadelphia, Pennsylvania 19174

ABSTRACT

The distribution of labeled RNA in the optic nerve of the rabbit was studied by quantitative ultrastructural autoradiography after the intraocular injection of [^{3}H]uridine. The highest density of silver grains related to [^{3}H]RNA (27–40 grains/100 μm^2) was found in glial cell perikarya; a slightly lower density was present in the glial nuclei (19–20 grains/100 μm^2). Axons (4–5 grains/100 μm^2) and myelin (2–3 grains/100 μm^2) had the lowest grain densities. 74–83% of all counted grains were located outside the axons. By comparing the grain density distribution over the axon with that expected in the case of an exclusive labeling of the surrounding myelin and glial cell processes, it was concluded that the axons contained a number of grains representing [^{3}H]RNA significantly higher than that expected to scatter from myelin and glial processes. Most of these grains were concentrated at the periphery of the axon and were not related to axonal mitochondria.

Previous studies on the axonal flow of RNA have shown that after the administration of RNA precursors to ganglion cells of the retina or to motor neurons of the spinal cord, in addition to RNA, there is also a considerable amount of precursors along the optic and sciatic nerves (1–3). These findings have raised the question as to whether RNA migrates from the ganglion cell bodies into the nerves by axonal flow or is synthesized locally within the nerves. Recently, we have obtained evidence that at least 70–80% of the labeled RNA present along the optic nerve after the intraocular injection of [^{3}H]uridine is synthesized within the optic nerve (4). On the basis of this and other findings (4), we have postulated that after intraocular injection, the RNA precursors migrate distally inside the axons from the ganglion cell bodies of the retina, and that during this migration, they are taken up by adjacent glial cells where they are incorporated into RNA (4). In the present study, we have investigated by ultrastructural autoradiography the localization of labeled RNA within the optic nerve after intraocular injection of tritiated uridine. The results indicate that 74–83% of the radioactivity related to labeled RNA is extra-axonal and that glial cell bodies are the most heavily labeled structures. A relatively small but significant amount of labeled RNA is found inside the axons.

MATERIALS AND METHODS

Albino rabbits weighing 2–2.5 kg were used. In the attempt to label the entire optic system, 50 μl containing 50 μCi of [5,6-^{3}H]uridine (New England Nuclear, Boston, Mass., 40–44 Ci/ml)

were injected into the eye on four (experiment 1) or five (experiment 2) consecutive days, and the animals were sacrificed after an overdose of Nembutal ,17 and 9 days, respectively, after the first injection. The optic nerves were dissected at 4°C and fixed either by immersion in 4% paraformaldehyde followed by postfixation in 1% osmium (experiment 1) or by immersion directly in 1% osmium (experiment 2) as reported in a previous study (4). To ensure that all the unincorporated precursor was released from the samples during fixation and that the radioactivity remaining in the tissue represented only labeled RNA, nerve segments from these, as well as from other animals similarly injected, were bisected longitudinally and weighed: one half of the nerve was extracted with 0.2 N $HClO_4$ and the amounts of acid-soluble and RNA-incorporated radioactivity determined as previously described (4); the other half was processed for electron microscopy (EM) and the fixatives were changed until there was no significant release of radioactivity. In all the experiments, the amount of radioactivity recovered during fixation accounted for 98–105% of that obtained in the acid-soluble fraction from the corresponding half of the nerve. Furthermore, homogenization of paraformaldehyde-fixed optic nerves with 0.2 N $HClO_4$ released less than 3% of the total radioactivity remaining after the multiple washes with the fixatives; subsequent treatment of the pellet with RNAse (1 mg/ml, at 37°C overnight) rendered virtually all of the remaining radioactivity acid soluble.

Autoradiograms for light and electron microscope examination were prepared (4, 5) with sections from the experimental (injected side) and control (uninjected side) nerves mounted on the same slide (4, 5). Some of the EM autoradiograms were latensified and developed with Elon ascorbic acid (6). Light microscope autoradiography was performed at different levels of the optic nerve, while the ultrastructural autoradiographic study was limited to segments taken 5–9 mm from the sclera. Random electron micrographs taken from 23 grids were enlarged to a final magnification of 30,000, checked by a grating replica (Ernest F. Fullam, Inc., Schenectady, N. Y.). Randomization of the electron micrographs was obtained according to the following procedure: at a magnification of 10,000, the squares of a 200-mesh grid can be divided into 100 electron microscope fields by the use of the graded stage controls of the Siemens Elmiskop IA. According to the fractional area of the square occupied by the section, 12–36 fields from one square for each grid were selected for photography, moving the stage controls according to coordinates selected from a table of random numbers (7). The EM autoradiograms were analyzed for the number of grains in each of the following seven compartments: (*1*) axons, (*2*) myelin, (*3*) glial cell nuclei, (*4*) glial perikarya, (*5*) glial processes, (*6*) blood vessels and collagen, and (*7*) unidentified structures and extracellular spaces. In addition to the perinuclear region, areas of cytoplasm measuring more than 2 μm in width were also considered to be part of the perikarya. However, the distinction between glial perikaryon and processes was often arbitrary. The fractional area of each compartment was calculated by the technique of random points (5, 8). The geometrical center of each silver grain present in the electron micrographs was determined and the grain was assigned to that compartment of the optic nerve over which its center fell. In order to introduce a partial correction for the scattered radiation from glial cell bodies, we excluded from the analysis grains and points falling outside these structures up to a distance of 1.3 μm (8 HD[1]) (5, 9, 10). At this distance, the density of grains representing "scatter" from a labeled source of infinite radius (as glial cell bodies may be considered) is <2.5% of the average density over the source (see Fig. 10 a and b of reference 9). The grain densities were calculated in the various compartments of both the experimental and control nerves. The densities found over the control nerves were considered as originating from background and were subtracted from the densities found over the experimental nerves.

The grain density distribution over the axon, and myelin and other surrounding structures at a distance up to 2 HD (experiment 1) or 3 HD (experiment 2) from the axolemma (Fig. 1), was obtained according to the techniques of Salpeter et al. (9, 10). These experimental grain density distributions were compared with the theoretical distribution expected if only the structures surrounding the axon were labeled. The theoretical model was a uniformly labeled annulus whose inner radius was equal to the average axon radius (3.5 HD), and its thickness was either 2 or 3 HD.

Data for the model annulus was obtained in the following way: the density values at ½ HD intervals from the center of five (experiment 1) or seven (experiment 2) concentric circular sources, with radius increasing from 3.5 to 5.5, or 6.5 HD, were determined from Fig. 9 of Salpeter et al. (9). Keeping a common center, the density values contributed by each circle at corresponding ½ HD intervals were added. Since in both experiments 1 and 2 the grain densities up to 2–3 HD outside the axon were uniform, the theoretical grain densities over the annulus

[1] HD is an experimental measure of resolution (see references 5, 9, and 10 for details). For this study, HD was approximately 1600 Å for autoradiograms developed with Microdol X and 1500 Å for autoradiograms developed with Elon ascorbic acid (6).

and the experimental grain densities outside the axon were normalized to one (11).

RESULTS

Light microscope autoradiograms showed that the majority of the silver grains were located in the septa separating bundles of axons (Fig. 2). The vessels of the septa were lightly labeled and a few grains were seen in the leptomeninges. Cross sections of the entire nerve showed no difference in the pattern of grain distribution between the central and peripheral zones or between the nasal and temporal halves. The pattern of grain distribution remained the same in the most distal segment (10–12.5 mm from the sclera), although at this level the grain density was much lower than in the proximal segments of the optic nerve. On electron microscope examination, the glial cell bodies appeared to be more heavily labeled than other structures (Fig. 3). Quantitative autoradiographic analysis (Table I) confirmed that in both experiments, the highest grain density was present in the glial perikarya and nuclei, while a lower grain density was found in the glial cell processes. The grain density over axons and myelin was almost 10 times lower than that over glial cell bodies.

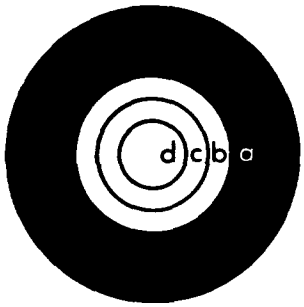

FIGURE 1 Diagram of the compartments analyzed for grain density distribution. (*a*) Extraaxonal compartment, (*b*, *c*, and *d*) intraaxonal compartments.

49–63% of all the grains were located over the glial cells, while only 17–26% were present over the axons (Table II). However, the grain density over the axons of the experimental nerve was more than 10 times greater than that over the axons of the control side (Table I), and 4–8 times greater than the grain density expected as "scatter" from adjacent glial cell bodies, indicating that the labeling of the axons was not due to background or to mere scattered radioactivity. In order to rule out the possibility that the grains present in the axons were due to scatter from the myelin sheath or adjacent glial cell processes, the grain densities inside and outside the axon

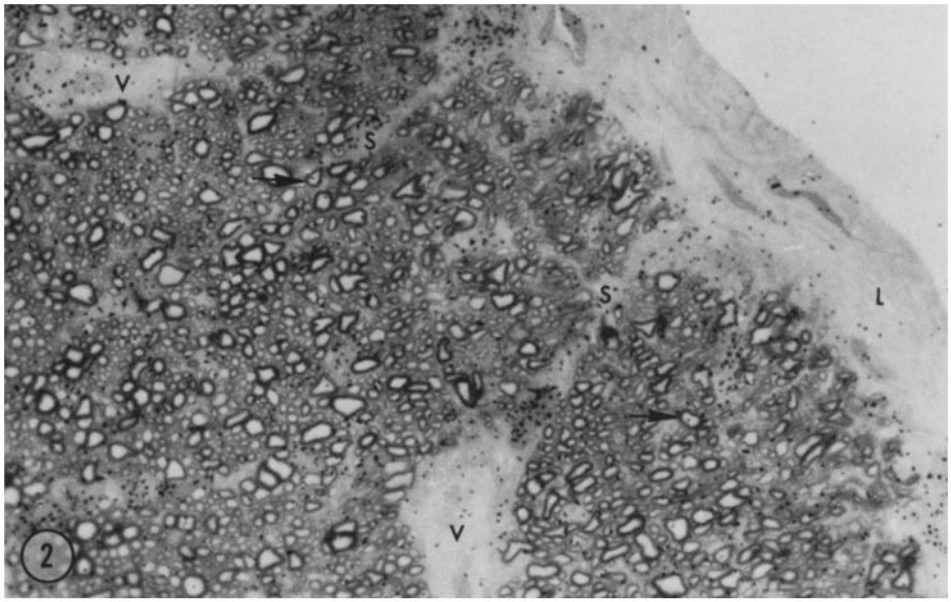

FIGURE 2 Light microscope autoradiograms of a cross section of the optic nerve (experiment 2). Most of the grains are in the septa (*S*). Blood vessels (*V*) and leptomeninges (*L*) contain relatively few grains. A few grains are located inside the axons (arrows). Stained with paraphenilendiamine. × 750.

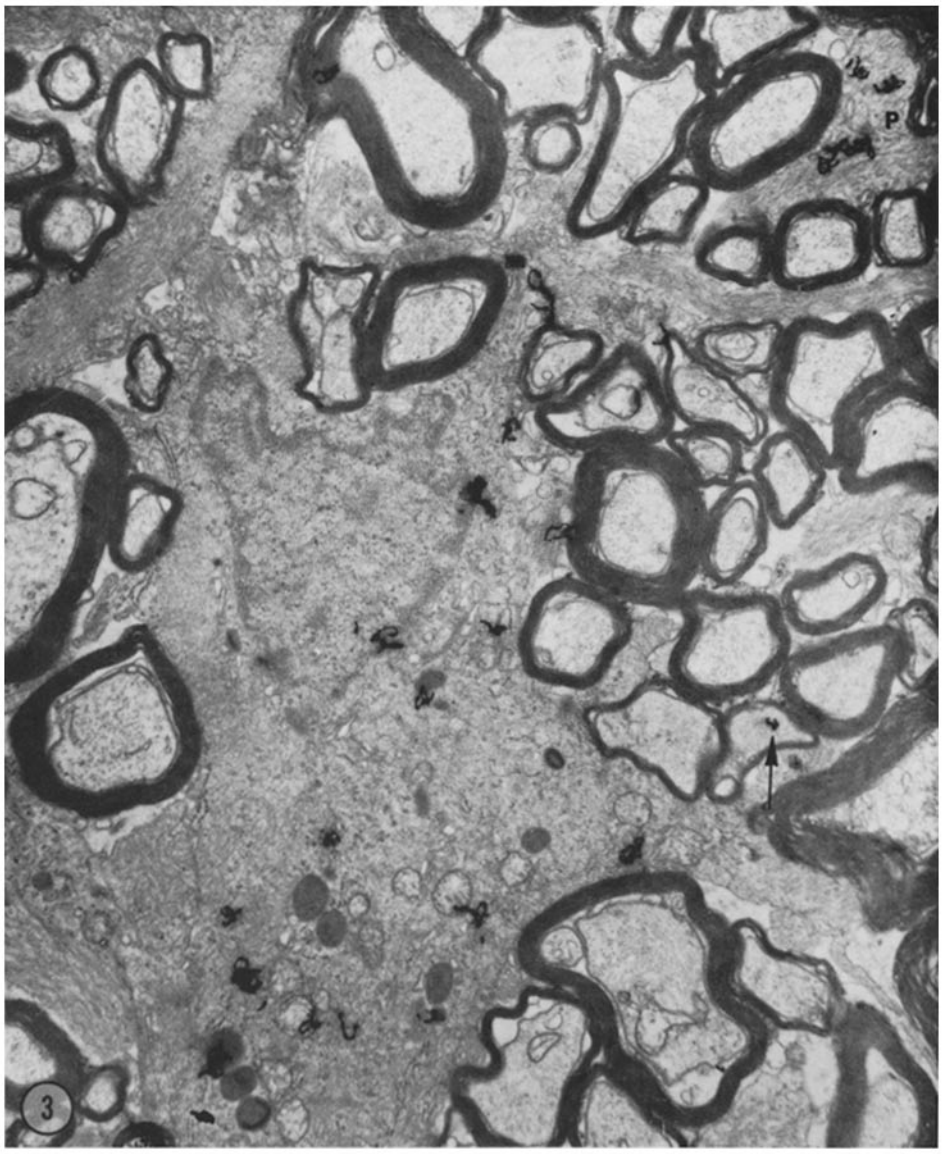

FIGURE 3 Electron microscope autoradiogram (experiment 2). Cross section of nerve showing several silver grains located over the perikarya of a glial cell, and over a glial cell process (*P*, upper right corner). The remaining grains are located over myelin. One grain is located over the axon (arrow). × 12,000.

at various distances from the axolemma (Fig. 1) were calculated and compared with those expected if the extraaxonal structures were the only source of the radioactivity. As shown in Table III, in both experiments 1 and 2, all the grain densities found inside the axon were significantly higher than those expected if only the surrounding extraaxonal structures had been labeled. The experimental intraaxonal grain densities decreased progressively from the periphery toward the center of the axon. These findings indicate that labeled RNA is present inside the axon and that the intraaxonal labeled RNA is located mainly at the periphery rather than at the center of the axon. The number of intraaxonal grains was not influenced by the presence of mitochondria since no difference in the grain density was found between axons containing and not containing mitochondria in the section (Table IV).

TABLE I

Grain Densities over Various Compartments of the Optic Nerve (Grains/100 μm²)

	Axon	Myelin	Glial			Vascular areas	Other*	Total nerve	Area surveyed (μm²)
			Processes	Perikarya	Nuclei				
Experiment 1	3.81 ±0.62 (0.31 ±0.18) [49]	2.36 ±0.47 (0.93 ±0.21) [62]	7.84‡ ±0.91 (0.39 ±0.19) [86]	39.61‡ ±5.06 (0.69 ±0.63) [69]	19.25‡ ±4.35 (0) [20]	4.80 ±1.80 (0) [7]	1.41 ±0.81 (0) [3]	5.66 ±0.38 (0.57 ±0.11) [296]	4755 (4772)
Experiment 2	4.92 ±0.65 (0.36 ±0.25) [78]	3.47 ±0.53 (0.36 ±0.26) [71]	5.99 ±0.80 (0.38 ±0.27) [73]	27.38‡ ±4.34 (0) [41]	20.49‡ ±4.85 (3.49 ±2.02) [30]	(0) [0]	1.28 ±0.74 (0) [0]	5.43 ±0.37 (0.46 ±0.15) [296]	5020 (1976)

Values represent densities on the injected side minus densities on the uninjected side (numbers in parenthesis). Values in brackets represent number of grains. Standard errors were obtained using the formula $G/P\sqrt{1/G + 1/P}$, where G = the number of grains and P = number of points (10).

* Extracellular spaces and unidentifiable structures.

‡ Significantly different ($P < 0.02$–0.001) from values for axon and myelin. The formula $D_1 - D_2/\sqrt{(SE_1)^2 + (SE_2)^2}$, where D = density and SE = standard error was used to determine the level of significance.

TABLE II

Percentage Grain Distribution

	Axon	Myelin	Glial cells	Vascular areas	Other*
Experiment 1	16.7	16.7	63.0	2.6	1.0
Experiment 2	26.4	23.2	49.3	—	1.1

Values have been corrected for background.

* Extracellular space and unidentified processes.

DISCUSSION

In any autoradiographic study intended to detect the presence and distribution of a substance within various components of a tissue, at least two conditions should be satisfied: (*a*) that the substance being studied is the only source of radioactivity in the tissue, and (*b*) that the silver grains located over a certain structure represent emissions from a radioactive source present within the structure. In the present experiments negligible amounts of radioactivity were extracted from the fixed tissues by homogenizing with 0.2 N $HClO_4$, and all the radioactivity remaining in the tissue was RNase sensitive. These findings indicate that the nonincorporated labeled precursors were removed during fixation and that RNA was the only radioactive source in the tissue. As for the second condition, Salpeter et al. (9) have shown that due to "scattering," a portion of the silver grains derived from a radioactive source will fall outside the source. This scatter will significantly affect compartments of the tissue that surround a larger and more heavily labeled structure, while the "cross scatter" of a neighboring compartment of similar size and radioactivity will cancel out the effect. We have therefore introduced a partial correction for the "scatter" from the glial cell bodies, the most heavily labeled structures, by not taking into account an area 1.3 μm (8 HD) wide around them. Beyond this distance, the grain density due to scatter from a source of infinite radius, as glial cell bodies may be considered, is less than 2.5% the average density over the source (see Fig. 10 a and b of reference 9). As shown in Table I, the grain densities found over the axons were about 10–20% of those found over the glial cell perikarya, i.e., the grain densities over the axons were more than 4–8 times higher than the densities expected in the case of mere scatter from adjacent glial cell perikarya. Therefore, even taking into consideration the unlikely possibility of occasional overlapping of the scatter from more than one glial cell body, it is clear that the radioactivity found over the axon could not be due only to scatter from glial cell perikarya. As for the scatter to the

TABLE III

Experimental and Expected Distributions of Grain Densities over Various Compartments of the Axon after Normalization of Densities over Surrounding Myelin and Glial Cell Processes

	Intraaxonal compartments			Surrounding myelin and glial processes*
Distance in HD from axolemma	2–3.5 (d)‡	1–2 (c)	0–1 (b)	(a)
Experiment 1				
Experimental densities	0.681 ± 0.173§	0.909 ± 0.149‖	1.394 ± 0.136¶	1.0 ± 0.075
Expected densities if only the surrounding structures were labeled	0.340	0.450	0.771	1.0
Experiment 2				
Experimental densities	1.112 ± 0.241‖	1.302 ± 0.213¶	1.663 ± 0.190¶	1.0 ± 0.083
Expected densities	0.370	0.474	0.759	1.0

Standard errors were determined as for Table I except that the values were multiplied by the same factor used to normalize the densities outside the axon. The formula (experimental density-expected density)/standard error was used to determine the level of significance.

* The grain densities over the structures surrounding the axons were determined up to a distance of 2 HD from the axolemma for experiment 1 and of 3 HD for experiment 2.

‡ See Fig. 1 for representation of compartments.

§ Significantly different from the expected densities ($P < 0.05$).

‖ Significantly different from the expected densities ($P < 0.01$).

¶ Significantly different from the expected densities ($P < 0.001$).

TABLE IV

Grain Densities over Axons (Grains/100 μm²)

With mitochondria*	Without mitochondria*
3.75 ± 1.01	3.97 ± 0.68

No background corrections were made.

* Refers to axons which contained or did not contain mitochondria in the autoradiograms.

axon from the surrounding myelin sheath and adjacent glial processes, the analysis of the grain density distribution showed that the grain densities over all the compartments inside the axon were significantly higher than that expected to scatter from the surrounding structures (Table III). On the other hand, the difference in grain density between glial perikarya and their nuclei and between glial processes and myelin sheaths did not seem great enough to require corrections. It can therefore be concluded that the grain densities found over the various structures are representative of the radioactivity present, and that the axons have been labeled.

The finding that 74–83% of the silver grains were located outside the axons, and that the glial cell bodies had by far the highest grain density, is consistent with the conclusion of our previous study (4) that after the intraocular injection of [³H]uridine, most of the RNA present in the optic nerve is synthesized locally in the glial cells. In addition, the present findings show that RNA is present in the axons; this RNA is concentrated mainly in the periphery of the axon and is not located only in mitochondria since axons containing and not containing mitochondria in the section had similar grain density (Table IV). Our results confirm the tentative conclusion of Peterson et al. (12), who in a light microscope study of the sciatic and optic nerves after intraspinal and intraocular injections of [³H]orotic acid, observed that the silver grains were located mainly in Schwann and glial cells, though some appeared to be located in axons. Also, the present study further substantiates the contention that RNA is present inside the axon (references 13 and 14 for review, and 15, 16). What is uncertain in our experiment is the origin of the RNA found inside the axon. Two possibilities may be considered. The first is that RNA has migrated intra-

axonally from the ganglion cell body of the retina. Recently, Bondy (17), working with the chick optic lobe, and Ingoglia et al. (18), using optic tectum of the goldfish after intraocular injection of labeled uridine, have obtained indirect evidence that RNA migrates along the axons of the optic pathways. It is possible, therefore, that the RNA we have detected inside the axons represents RNA that has migrated down the axons. Should this be the case, it would be difficult in our system to characterize its migration pattern because the small amount of axonal RNA (about 20%) would be masked by the larger quantity of locally synthesized extraaxonal RNA (4).

The second possibility is that all the RNA present in the optic nerve, including the intraaxonal RNA, is synthesized locally. This possibility has to be considered in view of the light microscope autoradiographic findings of Singer and Green (19) according to whom grains related to RNA are seen over the axons of the peripheral nerve of the *Triturus* after the intraperitoneal injection of [^{3}H]uridine; furthermore, transection of the nerve resulted in neither a change in the amount nor in the distribution of the radioactivity. These findings indicate that the peripheral nerve is able to synthesize RNA and that some of this locally synthesized RNA is present in the axon. Whether the intraaxonal RNA was synthesized in the adjacent glial cells and then transferred into the axon or synthesized in the axon itself was not determined by Singer and Green. Theoretically, the transfer of RNA from glial cells to axons is possible, since there is evidence that macromolecules may enter the axon from adjacent supporting cells and that intact RNA may be transferred from one cell to another cell (20–23). However, in view of the findings obtained by Edström et al. (24) and Koenig (25), the possibility that the axonal RNA is synthesized in the axon itself cannot be definitely ruled out.

Since both RNA and precursors are distributed as a steep gradient in the optic system, the distribution of labeled RNA along the optic nerve might differ from that in the more distal portions of the system. Further studies are underway to clarify this point.

The authors wish to thank Dr. Miriam Salpeter for her help in the analysis of grain density distribution, Dr. John de Cani for his advice in the statistical analysis, Dr. Nicholas K. Gonatas for his helpful comments.

This work was supported by U. S. Public Health Service grants NS 08933 and NS 05572-09 from the Division of Neuropathology, University of Pennsylvania, Philadelphia, Pa.

Received for publication 26 April 1973, and in revised form 3 August 1973.

REFERENCES

1. Austin, L., J. J., Bray, and R. J. Young. 1966. Transport of proteins and ribonucleic acid along nerve axons. *J. Neurochem.* **13**:1267–1269.
2. Casola, L., G. A. Davis, and R. E. Davis. 1969. Evidence for RNA transport in the rat optic nerve. *J. Neurochem.* **16**:1037–1041.
3. Bray, J. J., and L. Austin. 1968. Flow of protein and ribonucleic acid in peripheral nerve. *J. Neurochem.* **15**:731–740.
4. Autilio-Gambetti, L., P. Gambetti, and B. Shafer. 1973. RNA and axonal flow. Biochemical and autoradiographic study in the rabbit optic system. *Brain Res.* **53**:387–398.
5. Gambetti, P., L. Autilio-Gambetti, N. K. Gonatas, and B. Shafer. 1972. Protein synthesis in synaptosomal fractions. Ultrastructural radioautographic study. *J. Cell Biol.* **52**:526–535.
6. Salpeter, M. M., and M. Szabo. 1972. Sensitivity in electron microscope autoradiography. I. The effect of radiation dose. *J. Histochem. Cytochem.* **20**:425–434.
7. A Million Random Digits with 100,000 Normal Deviates. 1955. The Rand Corporation. Free Press, Publishers, Glencoe, Ill.
8. Salpeter, M. M. 1968. H^3-proline incorporation into cartilage. Electron microscope autoradiographic observations. *J. Morphol.* **124**:387–422.
9. Salpeter, M. M., L. Bachman, and E. E. Salpeter. 1969. Resolution in electron microscope radioautography. *J. Cell Biol.* **41**:1–20.
10. Budd, G. C., and M. M. Salpeter. 1969. The distribution of labeled norepinephrine within sympathetic nerve terminals studied with electron microscope autoradiography. *J. Cell Biol.* **41**:21–32.
11. Hedley-Whyte, E. T., F. A. Rawlins, M. M. Salpeter, and B. G. Uzman. 1969. Distribution of cholesterol-1,2-H^3 during maturation of mouse peripheral nerve. *Lab. Invest.* **21**:536–547.
12. Peterson, J. A., J. J. Bray, and L. Austin. 1968. An autoradiographic study of the flow

of protein and RNA along peripheral nerve. *J. Neurochem.* **15**:741–745.

13. EDSTRÖM, A. 1969. RNA and protein synthesis in Mauthner nerve fiber components of fish. *In* Cellular Dynamics of the Neuron. S. H. Barondes, editor. Academic Press, Inc., New York. 51–72.
14. KOENIG, E. 1969. Nucleic acid and protein metabolism of the axon. *In* Handbook of Neurochemistry. Vol. 2. R. Lajtha, editor. Plenum Press, New York. 423–434.
15. LASEK, R. J. 1972. Characterization of axoplasmic RNA from squid and polycheate giant axons. Transactions of the American Society for Neurochemistry. 3rd Annual Meeting. Seattle. 98.
16. AMALDI, P., and G. RUSCA. 1970. Autoradiographic study of RNA in nerve fibres of embryonic sensory ganglia cultured in vitro under NGF stimulation. *J. Neurochem.* **17**: 767–711.
17. BONDY, S. C. 1972. Axonal migration of various ribonucleic acid species along the optic tract of the chick. *J. Neurochem.* **19**:1769–1776.
18. INGOGLIA, N. A., B. GRAFSTEIN, B. S. MCEWEN, and I. G. MCQUARRIE. 1973. Axonal transport of radioactivity in the goldfish optic system following intraocular injection of labeled RNA precursors. *J. Neurochem.* **20**:1605–1615.
19. SINGER, M., and M. R. GREEN. 1968. Autoradiographic studies of uridine incorporation in peripheral nerve of the newt, Triturus. *J. Morphol.* **124**:321–343.
20. SINGER, M., N. KRISHNAN, and D. A. FYFE. 1972. Penetration of Ruthenium Red into peripheral nerve fibers. *Anat. Rec.* **173**:375–390.
21. GIUDITTA, A., B. D'UDINE, and M. PEPE. 1971. Uptake of proteins by the giant axon of the squid. *Nature (Lond.)*. **229**:29–30.
22. HOLTZMAN, E., and E. R. PETERSON. 1969. Uptake of proteins by mammalian neurons. *J. Cell Biol.* **40**:863–869.
23. KOLODNY, G. M. 1971. Evidence of transfer of macromolecular RNA between mammalian cells in cultures. *Exp. Cell Res.* **65**:313–324.
24. EDSTRÖM, A., J. E. EDSTRÖM, and T. HÖKFELT. 1969. Sedimentation analysis of ribonucleic acid extracted from isolated Mauthner nerve fibre components. *J. Neurochem.* **16**:53–66.
25. KOENIG, E. 1967. Synthetic mechanisms in the axon. IV. *In vitro* incorporation of H^3 precursors into axonal protein and RNA. *J. Neurochem.* **14**:437–446.